Growth of a two-dimensional Er silicide on Si(111)

P. Paki, U. Kafader, P. Wetzel, C. Pirri, J. C. Peruchetti, D. Bolmont, and G. Gewinner

Laboratoire de Physique et de Spectroscopie Electronique, Faculté des Sciences et Techniques, 4 rue des Frères Lumière, 68093 Mulhouse CEDEX, France

(Received 30 September 1991; revised manuscript received 12 November 1991)

Initial stages of $ErSi_{1.7}$ formation on Si(111) surfaces were investigated by means of low-energy electron diffraction, angle-resolved ultraviolet photoemission spectroscopy, and x-ray-photoelectron forward-scattering techniques. Experimental data are presented that demonstrate the formation of a $p(1\times1)$ ordered-surface silicide by deposition of one Er monolayer onto Si(111) held at room temperature and subsequently annealed at 550 °C. The structure of this two-dimensional compound appears to be similar to a single $ErSi_2$ layer (AlB_2 structure) with a reconstructed Si top layer.

Rare-earth-metal silicides have attracted wide interest both for technological and fundamental reasons. Besides the possibility of epitaxial growth on Si(111) they exhibit several interesting properties like formation of the lowest (highest) Schottky-barrier heights on *n*-type (*p*-type) Si, or their unusual magnetic behavior.[1,2] This study deals with the Er/Si(111) system which is attractive because of the relatively close match (1.5%) in surface translation vectors of $ErSi_{1.7}(0001)$ and Si(111). Epitaxial growth of $ErSi_{1.7}$ on Si(111) is therefore expected and actually observed.[2–7] The relevant epitaxial relationships are $ErSi_{1.7}(0001)\|Si(111)$ with $ErSi_{1.7}[\bar{1}010]\|Si[\bar{1}10]$ and $ErSi_{1.7}[12\bar{3}0]\|Si[11\bar{2}]$. In bulk form, it has been established by several authors that this phase presents a Si deficiency of about 15% with respect to the ideal hexagonal $ErSi_2$ (AlB_2-type) structure. This results from ordered vacancies in the Si sublattice (1.7 stoichiometry instead of 2). These vacancies order in a periodic array, giving rise to a $(\sqrt{3}\times\sqrt{3})R30°$ superstructure in the (0001) plane.

In this paper, we mainly concentrate on the very initial stage of Er silicide formation in the monolayer (ML) range. To this end, we have used standard surface-sensitive techniques such as low-energy electron diffraction (LEED) and angle-resolved ultraviolet photoemission spectroscopy (ARUPS) in conjunction with x-ray-photoelectron forward scattering (XPFS). This latter technique is described in detail in Refs. 8 and 9. Photoelectrons, having kinetic energies of the order of a few hundred electron volts, emitted by a specific atom, are scattered by the potential of a surrounding atom. This results in enhanced intensities in the forward-scattering (FS) direction, i.e., in the direction connecting the emitting atom to the scatterer. In practice the method gives straightforward information on bond directions connecting the emitter to its nearest neighbors.

The main result of our measurements is that a surface silicide phase displaying $p(1\times1)$ two-dimensional (2D) order can be grown by deposition of one Er ML on Si(111) held at room temperature (RT) and subsequently annealed at 550 °C. This 2D silicide consists of an ordered Er ML, covered with a Si layer. The atomic arrangement in the surface silicide closely resembles a single $ErSi_2$ (AlB_2-structure) layer but with a reconstructed Si top layer.

Experiments were performed in an ultrahigh vacuum system (base pressure below 10^{-10} Torr) comprising a growth chamber and an analysis chamber equipped with facilities for XPS, ARUPS, and LEED techniques. The photoelectrons were analyzed with a hemispherical analyzer set at a half-acceptance angle of 1°. For XPFS studies the Er 4*f* intensities were collected with Mg $K\alpha$ excitation ($h\nu=1253.6$ eV) as a function of polar angle θ (angle defined with respect to the normal to the surface) in a selected azimuthal plane. The experimental error in the angular position of the XPFS structures is about $\pm1°$. The UPS studies were carried out with He II ($h\nu=40.8$ eV) radiation to take advantage of the very good energy resolution (~0.2 eV) and large photoionization cross section of the corelike Er 4*f* multiplet. All the photoemission data were taken in a geometry with a fixed angle (65°) between the photon source and the electron analyzer. The Si(111) sample surface was cleaned by repeated cycles of argon-ion bombardment followed by high-temperature annealing (800 °C). Er was evaporated from a boron-nitride crucible heated by an electron beam. The Er flux, monitored with a quartz microbalance, as well as the relative Er and Si XPS intensities, was adjusted to give a deposition rate of ~1 ML/min [one ML corresponds to the Si(111) surface atomic density, i.e., 7.8×10^{14} atoms/cm^2]. An extensive source outgassing allowed us to maintain the residual pressure below 2×10^{-10} Torr during evaporation.

Figure 1 shows the valence-band spectra recorded with He II radiation at normal emission ($\theta=0°$) from different systems: 1 Er ML deposited on Si(111) (a) before and (b) after annealing at 550 °C; (c) 2 Er ML deposited at RT, then annealed at 600 °C and (d) a 60-Å-thick epitaxial $ErSi_{1.7}$ layer. The epitaxial $ErSi_{1.7}$ film was prepared as described previously[7] by thermal treatment at 700 °C of a 15-ML Er deposit onto clean Si(111). In this way, epitaxial film growth is achieved as evidenced by a sharp

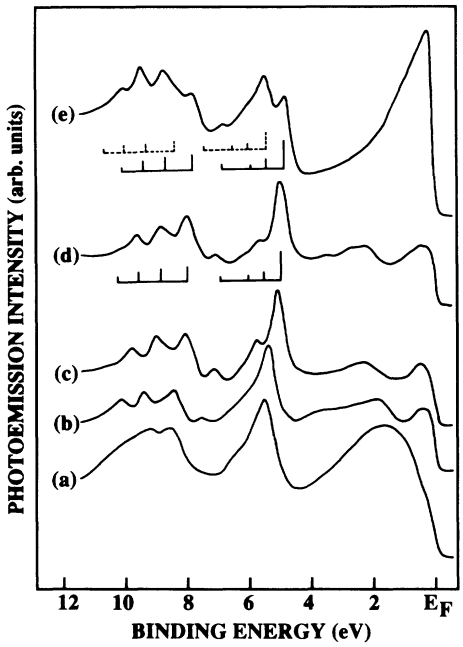

FIG. 1. Normal-emission valence-band spectra taken with He II ($h\nu$=40.8 eV) radiation for different systems: (a) 1 Er ML deposited on Si(111) at RT and followed by annealing at 550 °C; (b) and (c) 2 Er ML deposited on Si(111) at RT and subsequently annealed at 550 °C; (d) 60-Å-thick epitaxial $ErSi_{1.7}$ layer, and (e) pure Er layer. Also shown as insets are the identification of the bulk (full-line vertical bars) and surface (dashed-line bars) $4f$ multiplet components.

$(\sqrt{3}\times\sqrt{3})R30°$ LEED pattern and characteristic photoemission spectra.[7] Note that the $(\sqrt{3}\times\sqrt{3})R30°$ LEED pattern is still observed for coverages as low as 2 Er ML in the 400–600 °C annealing temperature range. Also shown is (e) the spectrum measured on a pure Er film. All these valence-band spectra are essentially dominated by Er $4f$ multiplet emission in the 4–11 eV binding-energy (BE) range. For spectra (a), (b), (c), and (d) the features located at ~2–3-eV BE are attributed to bonding states of mixed Si $3sp$-Er $5d$ orbitals while the peak near the Fermi level (~0.4 eV) reflects mainly Er $5d$ emission. It was shown in a previous work[10] that the BE of the Er $4f$ levels strongly depends on the local environment of the Er atoms. The spectrum recorded on pure Er exhibits both bulk and surface Er $4f$ emission.[11] This results in the presence of an additional multiplet reflecting emission from surface Er species and shifted by 0.7 eV toward higher BE's. In contrast, we found no evidence for the presence of surface Er sites on epitaxial crystalline $ErSi_{1.7}$ and concluded that $ErSi_{1.7}(0001)$ is terminated at least by one Si plane.[7,10] The relevant series of $4f$ multiplets in the case of $ErSi_{1.7}$ silicide as well as pure Er metal are shown as insets in Fig. 1.

For 1 Er ML deposited on Si(111) at RT, the valence-band spectrum [Fig. 1(a)] exhibits a fairly broad unresolved structure in the 7–11-eV BE window assigned to the contribution of different Er atomic environments, giving rise to a distribution of $4f$ lines with different BE locations. The LEED observations show that the (7×7) superstructure is destroyed and only a blurred (1×1) diagram persists at this stage, indicating a rather disordered overlayer. Yet, after annealing at 550 °C, the surface displays a $p(1\times1)$ LEED pattern with sharp spots and very low background intensity.

Furthermore, it can be seen in Fig. 1(b) that the $4f$ multiplet features become well resolved and shift slightly towards the Fermi energy. A striking similarity is now observed between the relevant spectrum and that collected on bulk $ErSi_{1.7}$ as far as the number, the relative intensities, and overall shape of the $4f$ multiplet components are concerned. The same statement holds for the mixed Er $5d$–Si $3s3p$ valence states in the 0–4-eV BE range. These observations indicate that a well-defined ordered silicide is formed where all Er atoms have a single atomic environment which must be very similar to the atomic arrangement in bulk $ErSi_{1.7}$. A possible interpretation may be that, already by 1 ML Er, three-dimensional bulklike epitaxial $ErSi_{1.7}$ islands are grown under the present annealing conditions. Yet, as shown below, this is definitely not the case and a 2D silicide, resembling a flat single $ErSi_2$ layer, is formed instead. First, if bulklike $ErSi_{1.7}$ were formed one should observe a $(\sqrt{3}\times\sqrt{3})R30°$ LEED diagram as opposed to the sharp $p(1\times1)$ pattern actually observed. The latter also suggests that no bare Si(111)(7×7) surface is left at this stage and the whole surface is coated with silicide. Second, the Er $4f$ BE in bulk $ErSi_{1.7}$ is about 0.4 eV higher than observed in the structure obtained by annealing 1 ML Er. In fact, it is apparent in Fig. 1 that the Er $4f$ levels shift progressively toward lower BE's with increasing silicide thickness or Er coverage. The limiting bulk value is practically observed for Er coverages above 5 ML (i.e., a 20-Å $ErSi_{1.7}$ silicide layer). This behavior indicates that the BE change is related to thin-film effects such as reduced final-state screening, increased Fermi energy due to quantization along the surface normal in ultrathin films,[12] or structural changes in the very early stages of silicide growth. Apparently, the silicide grows in a layer-by-layer mode and, in particular, 1 ML Er annealed at 550 °C lies flat on the substrate in the form of a 2D silicide.

Actually, strong support for this mode of growth comes from XPFS measurements. Figures 2(a) and 2(b) illustrate the Er $4f$ photoemission intensity polar angle distribution for various systems along the two symmetry directions ($[\bar{1}\bar{1}2]$ and $[\bar{1}10]$) of the Si(111) surface. Figure 2(a), curve (a) and 2(b), curve (a) display the XPFS patterns recorded for 1 Er ML deposited on Si(111) at RT. They are essentially featureless and identical to the instrumental response function, indicating an isotropic distribution of the Er $4f$ photoelectron intensity. Consequently, there are apparently no overlying Er or Si atoms scattering the photoelectrons from Er emitters. This indicates the presence of an essentially flat Er layer on top of the Si(111) surface. Alternatively, a completely disordered overlayer would also be compatible with the absence of FS features. Most remarkable, upon annealing at 550 °C the only change observed in the XPFS data occurs along a specific azimuthal orientation. Indeed, strongly enhanced emission appears at θ=40° along the

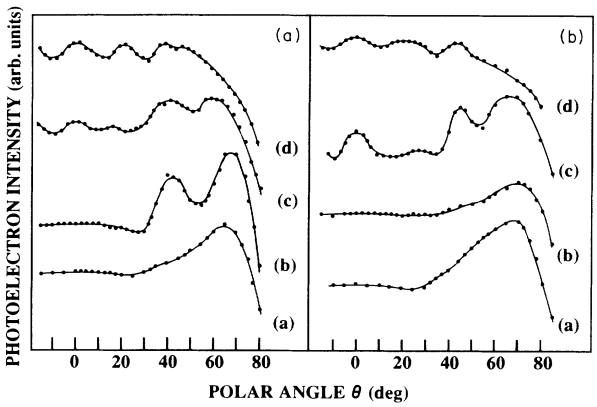

FIG. 2. Er $4f$ photoemission intensity vs polar angle along (a) the $[12\bar{3}0]$ $ErSi_{1.7}$ (or $[\bar{1}\bar{1}2]$ Si), (b) the $[\bar{1}010]$ $ErSi_{1.7}$ (or $[\bar{1}10]$ Si) azimuth from 1 Er ML deposited on Si(111) before RT [curve (a)] and after annealing at 550 °C [curve (b)]; 2 Er ML deposited on Si(111) at RT and subsequently annealed at 550 °C [curve (c)]; 60-Å-thick epitaxial $ErSi_{1.7}$ layer [curve (d)].

$[\bar{1}\bar{1}2]$ azimuth, while the $4f$ photoemission intensity remains quite isotropic along the $[\bar{1}10]$ azimuth. Note that the presence of a strong peak near 70° is mainly a feature of the instrumental response function, characteristic of a flat overlayer with a thickness in the ML range.[8] Actually, the lack of any FS peak along the $[\bar{1}10]$ azimuth indicates the absence of scatterers above the Er emitters along this azimuth. Hence, after annealing all the Er must still be close to the surface, probably below one (or possibly two) Si planes. Note, in particular, the absence of FS at normal emission, i.e., the absence of any scatterer just above the Er atoms. Again, this rules out the formation of three-dimensional silicide islands at this stage. Thus, the XPFS data confirm that upon annealing a specific structural change takes place where the Er are incorporated in an ordered surface compound. In order to gain more insight into the $p(1\times1)$ surface silicide structure we have carried out XPFS measurements on bulklike $ErSi_{1.7}$. The relevant XPFS patterns [Figs. 2(a), curve (d) and 2(b), curve (d)] are clearly dominated by FS features at $\theta=0°$, 21.4°, 38.5°, and 47° along the $[12\bar{3}0]$ azimuth and $\theta=0°$, 24.8° and 42.8° along the $[\bar{1}010]$ azimuth. To determine their origin, we now consider the AlB_2 structure and identify a set of low-index directions, which can contribute to the FS intensity maxima. The bulk $ErSi_2$ crystallographic AlB_2 structure consists of two kinds of basal planes, which are Si or Er, respectively, piled up alternatively parallel to the Si(111) substrate planes. The geometry of the $ErSi_2$ structure in the two high-symmetry $(12\bar{3}0)$ and $(\bar{1}010)$ planes probed in our experiments along the $[\bar{1}010]$ and $[12\bar{3}0]$ azimuths, respectively, is depicted in Fig. 3. It is apparent that for Er core levels, FS should occur at normal emission ($\theta=0°$) and $\theta=47°$ along the $[12\bar{3}0]$ azimuth, and at $\theta=43°$ along the $[\bar{1}010]$ azimuth. Clearly the experiments show all these peaks which correspond to scattering from nearest Er (Si) neighbors along $[\bar{1}010]$ ($[12\bar{3}0]$). The features shown at 21.4° along the $[12\bar{3}0]$ azimuth and 10°–30° along the $[\bar{1}010]$ azimuth are associated with next-nearest

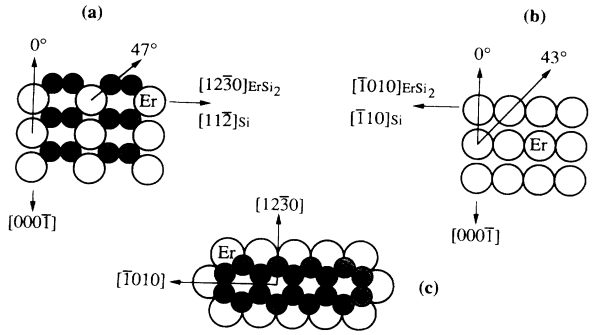

FIG. 3. Side views of the ideal $ErSi_2$ (AlB_2) structure corresponding to (a) the $[12\bar{3}0]$, (b) the $[\bar{1}010]$ azimuths. The arrows indicate the expected FS directions. (c) Top view of the $ErSi_2$ structure in the $[000\bar{1}]$ direction. The $ErSi_{1.7}$ bulk structure is the same except for the presence of ordered vacancies in the Si planes.

neighbors or more complex diffraction features. However, it turns out that the peak located at 38.5° along the $[12\bar{3}0]$ azimuth is not consistent with the simple AlB_2 structure. In this respect, our XPFS results can be directly compared to a study of thick $YSi_{1.7}$ films on Si(111) carried out by Baptist *et al.*[13] $YSi_{1.7}$ also crystallizes in the AlB_2 structure and grows epitaxially on Si(111). From their detailed analysis based on scattering calculations they conclude that the data are consistent with the AlB_2 structure of bulk $YSi_{1.7}$ but the (0001) surface exhibits a buckled Si top layer characterized by the presence of an additional FS peak at $\theta=39°$ in the Y $3d$ intensity versus polar angle curve along the $[12\bar{3}0]$ azimuth. This surface geometry, similar to the double layer on the ideal Si(111) (1×1) surface, is obtained by a displacement upward (0.7 Å) of one out of two Si atoms within the top (0001) Si termination of bulk YSi_2 [Fig. 3(c)]. Since our XPFS curves for $ErSi_{1.7}$ are quite identical to those for $YSi_{1.7}$ we conclude that bulk $ErSi_{1.7}$ silicide with AlB_2 structure is indeed formed in our experiment but with a top layer that is reconstructed with respect to the ideal AlB_2 structure according to the model proposed in Ref. 13.

Now, coming back to the structure of the surface silicide formed at 1 ML Er coverage, we show that a model made of a single $ErSi_2$ layer [Fig. 3(c)] similar to the reconstructed top layer on bulk $ErSi_{1.7}(0001)$ explains our XPFS data. Obviously, such a model readily accounts for the absence of any FS features along $[\bar{1}10]$ since there is no scatterer above the Er in the relevant plane. On the other hand, the characteristic feature observed at 40° along $[\bar{1}\bar{1}2]$ is attributed to scattering by Si in the top layer. This layer must be reconstructed since the FS peak is located at 40° rather than 47° in the ideal AlB_2 structure. Apparently this reconstruction is very similar to that observed on bulk $ErSi_{1.7}$ since for the latter the FS feature associated with the reconstructed Si top layer is located at $\theta=39°$. This peak reflects scattering from Si atoms displaced upwards with respect to their bulk position. In principle the surface Si atoms remaining in their bulk position also induce a specific FS feature at $\theta=47°$ along the opposite $[11\bar{2}]$ azimuth. On bulk $ErSi_{1.7}$ this feature can-

not be distinguished from the relevant peak due to emission from Er located in deeper layers with a bulklike Si environment. The absence of this peak in XPFS curves of the surface silicide indicates that either the two features associated with the two types of Si atoms are note-resolved in our data (note that the angular width of the 40° peak is about 14°, as opposed to ~10° for a typical FS feature on bulk $ErSi_{1.7}$) or that only one domain out of the two possible orientations of the surface silicide is actually formed. The $p(1\times1)$ LEED pattern indicates that the reconstructed surface Si(0001) plane does not involve Si vacancies. This is not surprising since the compression of the Si atoms in the bulk $ErSi_{1.7}$(0001) plane (Si-Si distance of 2.2 Å) favoring the formation of vacancies is removed in a buckled Si double layer similar to bulk Si (Si-Si distance of 2.35 Å).

Strong support for this interpretation of the XPFS curves for the surface silicide comes from the relevant data measured for 2 ML of Er annealed at 550 °C. Moreover, in the monolayer range the data nicely demonstrate the layer-by-layer growth mode of $ErSi_{1.7}$ on Si(111). Indeed, Fig. 2 shows a sharp transition between the XPFS curves for 1 and 2 ML of Er annealed at 550 °C. For 2 ML, prominent features at $\theta=0°$ and 45.7° along $[\bar{1}010]$ are now visible, clearly indicating the formation of a *second* $ErSi_2$ layer. At this stage the XPFS curve already closely resembles those measured on a bulklike $ErSi_{1.7}$-thick film. Moreover LEED now shows a definite $(\sqrt{3}\times\sqrt{3})R30°$ pattern characteristic of the ordered Si vacancies in bulk $ErSi_{1.7}$. This suggests that a bulklike (0001) Si plane sandwiched between the two Er planes is actually formed at this stage. A major point here is that this 2-ML film also exhibits the characteristic feature at 40° along $[12\bar{3}0]$. This is just the expected behavior if this peak indeed reflects the reconstructed Si top layer, as inferred from the discussion of the surface silicide data. Finally, a systematic shift of the FS features from their positions on thick films is observed. For instance, at 2 ML the Er-Er FS peak occurs at 45.7°, as opposed to 43° observed on thick layers. This suggests a contraction of the interlayer spacing in ultrathin films, possibly related to the expansion of pseudomorphic $ErSi_{1.7}$ in the (0001) plane because of the 1.5% lattice mismatch with Si(111).

In summary, we have investigated the initial stages of Er silicide formation on Si(111) by LEED, ARUPS, and XPFS techniques. Our data clearly establish that deposition of one Er ML on Si(111) at RT, followed by annealing at 550 °C, leads to the formation of a $p(1\times1)$ 2D silicide. This silicide adopts a structure resembling a single $ErSi_2$ layer (AlB_2 structure) with a reconstructed Si top layer. The reconstruction is very similar to the one proposed on the $YSi_{1.7}$(0001) surface, i.e., a buckled Si double layer as in bulk Si. Finally we find that bulk $ErSi_{1.7}$(0001) is terminated in the same way as bulk $YSi_{1.7}$(0001), as one might expect from their similar electronic and crystallographic structures.

The Laboratoire de Physíque et de Spectroscopie Electronique is "Unité Associée au Centre National de la Recherche Scientifique No. 1435."

[1]H. Noorde, J. de Sousa Pires, F. M. d'Heurle, F. Pasavento, C. S. Petersson, and P. A. Tove, Appl. Phys. Lett. **38**, 865 (1981).

[2]K. N. Tu, R. D. Thomson, and B. Y. Tsaur, Appl. Phys. Lett. **38**, 626 (1981).

[3]J. A. Knapp and S. T. Picraux, in *Thin Films—Interfaces and Phenomena,* edited by R. J. Nemanich, P. S. Ho, and S. S. Lau, MRS Symposia Proceedings No. 54 (Materials Research Society, Pittsburgh, 1986), p. 261.

[4]F. A. d'Avitaya, A. Perio, J. C. Oberlin,Y. Campidelli, and J. A. Chroboczek, Appl. Phys. Lett. **54**, 2198 (1989), and references therein.

[5]M. P. Siegal, F. H. Kaatz, W. R. Graham, J. J. Santiago, and J. van des Spiegel, Appl. Surf. Sci. **38**, 162 (1989).

[6]C. d'Anterroches, P. Perret, F. A. d'Avitaya, and J. A. Chroboczek, Thin Solid Films **184**, 349 (1990), and references therein.

[7]P. Wetzel, L. Haderbache, C. Pirri, J. C. Peruchetti, D. Bolmont, and G. Gewinner, Surf. Sci. **251/252**, 799 (1991).

[8]C. S. Fadley, Prog. Surf. Sci. **16**, 275 (1984).

[9]W. F. Egelhoff, Jr., Solid State Mater. Sci. **16**, 313 (1990).

[10]P. Wetzel, L. Haderbache, C. Pirri, J. C. Peruchetti, D. Bolmont, and G. Gewinner, Phys. Rev. B **43**, 6620 (1991).

[11]F. Gerken, A. S. Foldström, J. Barth, L. I. Johanson, and C. Kunz, Phys. Sci. **32**, 43 (1985).

[12]L. Haderbache, P. Wetzel, C. Pirri, J. C. Peruchetti, D. Bolmont, and G. Gewinner, Phys. Rev. B **39**, 1422 (1989).

[13]R. Baptist, S. Ferrer, G. Grenet, and H. C. Poon, Phys. Rev. Lett. **64**, 311 (1990).

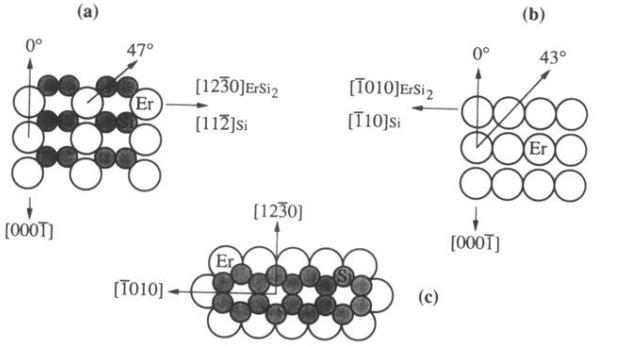

FIG. 3. Side views of the ideal $ErSi_2$ (AlB_2) structure corresponding to (a) the [12$\bar{3}$0], (b) the [$\bar{1}$010] azimuths. The arrows indicate the expected FS directions. (c) Top view of the $ErSi_2$ structure in the [000$\bar{1}$] direction. The $ErSi_{1.7}$ bulk structure is the same except for the presence of ordered vacancies in the Si planes.